

RESEARCH ARTICLE | DECEMBER 23 2024

Influence of amplitude and harmonic frequencies on the velocity of Faraday superwalkers

Pranav P P (प्रणव पी पी); Pranay Prabha Badvelu (प्रणय प्रभा बडवेलु) ; Venugopal Arumuru (वेणुगोपाल अरुमुरु)  



Physics of Fluids 36, 122142 (2024)

<https://doi.org/10.1063/5.0241020>



View
Online



Export
Citation

Articles You May Be Interested In

Infinite-memory classical wave-particle entities, attractor-driven active particles, and the diffusionless Lorenz equations

Chaos (January 2024)

Dynamics, interference effects, and multistability in a Lorenz-like system of a classical wave-particle entity in a periodic potential

Chaos (March 2023)

Introduction to focus issue on hydrodynamic quantum analogs

Chaos (September 2018)

Influence of amplitude and harmonic frequencies on the velocity of Faraday superwalkers

Cite as: Phys. Fluids **36**, 122142 (2024); doi: [10.1063/5.0241020](https://doi.org/10.1063/5.0241020)

Submitted: 28 September 2024 · Accepted: 3 December 2024 ·

Published Online: 23 December 2024



[View Online](#)



[Export Citation](#)



[CrossMark](#)

Pranav P P (प्रणव पी पी), Pranay Prabha Badvelu (प्रणय प्रभा बडवेलु), and Venugopal Arumuru (वेणुगोपाल अरुमुरु)^{a)}

AFFILIATIONS

Applied Fluids Group, School of Mechanical Sciences, Indian Institute of Technology Bhubaneswar, Khordha 752050, India

^{a)}Author to whom correspondence should be addressed: venugopal@iitbbs.ac.in

ABSTRACT

Faraday waves, arising from the vertical oscillation of a liquid bath, have long fascinated researchers for their role in studying non-equilibrium phenomena. The recent discovery of “superwalkers,” which are millimeter droplets exhibiting parabolic bouncing with high velocities on a vibrating liquid bath, has shown wave-particle interactions beyond classical theories. This study systematically investigates how key forcing parameters, such as the amplitude ratio, harmonic frequency, and phase angle difference between the dual-frequency excitation input signals, affect the velocity and walking dynamics of these superwalking droplets on a narrow straight channel. Experiments were performed using a mechanically vibrated silicone oil bath, with droplet motion tracked via a camera and particle-tracking algorithms. The investigated harmonic frequency pairs are (40, 80) Hz, (50, 100) Hz, and (70, 140) Hz, with amplitude ratios incrementally varied from 1 to 4.5 and phase angle differences between 120° and 150°. Results demonstrate a direct proportionality between amplitude ratio and droplet velocity, achieving velocities exceeding 60 mm/s for 1.9–2 mm droplets, surpassing previously reported results. Notably, the harmonic frequency determined the effective droplet size range exhibiting superwalking behavior. Higher frequencies limited mobility to smaller droplets (0.7–1.6 mm), while allowing initially stationary droplets to walk at substantial velocities. Conversely, lower frequencies enabled walking for larger droplets up to 2 mm. To explain these complex dynamics, a new correlation parameter (a/f^{15}) was formulated, revealing a linear relationship with droplet velocity across all frequencies and diameters investigated. The established quantitative relationships will be useful for precise control over droplet dynamics, enabling potential applications in microfluidics, surface manufacturing, and exploratory quantum analogy.

Published under an exclusive license by AIP Publishing. <https://doi.org/10.1063/5.0241020>

NOMENCLATURE

a	Acceleration
A	Amplitude
a_b	Threshold acceleration for bouncing
a_f	Faraday threshold acceleration
a_w	Threshold acceleration for walking
d	Diameter
f	Frequency in Hz
g	Acceleration due to gravity
g^*	a/g
t	Time
v	Velocity

Greek Symbols

ω	Angular velocity
ϕ	Phase angle difference

λ	Faraday wavelength
σ	Surface tension
ρ	Density

I. INTRODUCTION

Faraday instability, also known as the Faraday wave phenomenon, is an intricate hydrodynamic phenomenon that leads to the formation of standing waves on the surface of the fluid when a fluid-filled container is subjected to vertical vibrations.¹ This dynamic instability leads to the self-organization of energy and matter, which have fascinated researchers for decades due to their pivotal role in understanding non-equilibrium physical systems.² These Faraday waves have potential applications in micro-sized droplet generation, droplet control, manipulation, and mixing enhancement applications to name a few.^{3,4}

Faraday ripples, or Faraday waves, were first observed by Faraday¹ in 1831, and they observed the square patterns and

concluded that the vibrations are subharmonic. The first theoretical analysis was done by Benjamin and Ursell⁵ for ideal liquids enclosed in a container, vibrating sinusoidally in the vertical plane, and showed that the fluid dynamical equations can be reduced to a system of Mathieu equations. Kumar and Tuckerman^{6,7} did the first linear stability analysis for single-fluid problems and double-layer fluid problems. Even though initial experiments were capturing square patterns, recent experiments were able to capture multiple folded patterns using multiple frequency forcing.⁸ In the experiments done by Arbell and Fineberg⁸ on two-frequency forcing they were able to introduce new patterns with multiple wavelengths, which were not reported earlier. More intricate patterns with multiple wavelengths were produced when the bath was excited with multiple frequencies.

Interesting applications of Faraday waves were reported by Couder *et al.*⁹ in which they discovered that droplets of the same liquid can be made to bounce on the liquid bath without coalescence. They noticed that when vibrated above particular frequencies above a threshold acceleration (bouncing threshold), the droplet never makes contact with the liquid layer. A thin layer of air acts as a lubricating layer at the lowest point and the droplet gets detached at the highest position of the liquid bath. This process is repeated, and the droplets of a particular diameter range keep bouncing on the liquid bath indefinitely. The vibrations make it possible to delay the coalescence and let the droplets bounce on the bath.

The emergence of walking droplets, also known as pilot-wave systems, on a liquid bath undergoing Faraday instability, has provided a fascinating avenue for studying wave-particle interactions.¹⁰ A study conducted by Molacek and Bush^{11,12} on bouncing droplets and walking droplets gave a deeper understanding through experimental study and mathematical modeling of the phenomenon. Experiments showed that different bouncing modes were present depending on the number of times the droplet made contact with the liquid bath during the upward motion of the liquid bath. It was concluded that the walking of the liquid droplet was possible in a particular bouncing mode (2, 1) where the droplet makes contact with the liquid bath once for every two time periods of the bath.

Experiments using moving droplets have successfully mimicked quantum particle behavior, such as the single-slit experiment, the quantum corral, and quantum tunnelling.^{13–15} This behavior of droplets represents a hydrodynamical analogy of the quantum particles. Experiments have been done to manipulate the trajectory of the moving droplets as well as the velocity of the droplets. An interesting research was done to confine the droplet trajectory in a straight line, which was successful by making use of narrow channels within the vibrating container.¹⁶ It was shown that the droplets can be made to move in straight lines by submerged obstacles, which leads to unlocking further applications in droplet transport.

Valani *et al.*¹⁷ discovered that superwalkers, a recent revelation in this field, represent walking droplets that exhibit behaviors of classical wave-particle duality. Superwalkers are droplets with a diameter above 1 mm, which move at higher velocities. These walking droplets emerge when the liquid bath is forced with two frequencies with some particular phase difference. Droplets of this size range did not move when forced with a single frequency. However, they exhibit much higher velocities when subjected to the dual-frequency forcing, with reported maximum velocities of 50 mm/s for 2 mm droplet diameter. Another interesting behavior shown by these superwalkers was stop-and-go

locomotion when phase difference changes slowly with time. Valani *et al.*¹⁸ uncovered three different types of droplet motion: back-and-forth, forth-and-back, and irregular stop-and-go motion.

In recent investigations by Valani *et al.*,¹⁹ the influence of phase angle difference of excitation frequency pair on superwalkers along with mathematical explanation has been explored. They identified the amplitude difference in adjacent peaks influenced superwalking characteristics. Building upon this foundation, we try to explore more parameters that control the peak-to-peak difference of the input signal. In this regard, by systematically varying the amplitude ratio, harmonic frequency pair, and phase difference, we tried to quantify the effects on the behavior of these superwalkers.

The investigations by Valani *et al.*¹⁹ were mainly focused on understanding the influence of phase angle difference but preliminary findings in the existing literature suggest that multiple frequency forcing also significantly influences the patterns formed by these droplets, prompting an extended exploration of the role of amplitude, phase angle difference, and harmonic frequency in shaping the observed phenomena. The data available on the moving droplets are restricted to (80, 40) Hz harmonic frequency and are insufficient to make any conclusions about the effect of harmonic frequency on the droplet movement. Also, the effect of the amplitude ratio along with the combination of harmonic frequency and phase angle difference are yet to be explored. Hence, the primary objective of this study is to understand how factors like harmonic frequency, amplitude ratio, and phase angle difference affect superwalker behavior, by systematically varying these parameters.

The study seeks to give insights into the optimum parameters to control the droplets with the maximum possible velocity in narrow linear channels. Experiments conducted in narrow channels provide valuable insights into the boundary effects on walking droplets, which are crucial for applications involving droplet transport. Additionally, maintaining uniform vibrations is more feasible in a narrow channel setup, ensuring consistent experimental conditions.

II. EXPERIMENTAL METHODOLOGY AND DATA ACQUISITION

The experimental setup includes the MB Dynamics modal 50 shaker and a function generator with a two-channel output that gives the electrical signal input to the shaker. The function generator allows for exact control over the signal's amplitude, frequency, and phase angle differences. To verify the output signal combined from the function generator's two channels, an oscilloscope was used. After being amplified, the electrical signal is fed to the mechanical shaker. The harmonic frequency and phase angle differences are controlled by the function generator, while the amplitude is regulated through both the function generator and the amplifier gain.

A square aluminum cavity of 120 mm × 120 mm is fabricated with a narrow channel of 10.6 mm width and 3 mm depth at the middle of the aluminum plate.¹⁶ A top view of the narrow channel with the droplet captured during experiments is shown in Fig. 1. The channel is painted with matt black for better contrast of image during video capturing. The container is mounted on the vibration shaker and leveled with the help of an accurate spirit level.

In the present experiment, 20 cSt silicone oil is used as the working fluid. The oil is filled to a depth of 3 mm in the narrow channel and to less than 1 mm outside the channel. The narrow channel serves as a submerged boundary, while the thin oil layer outside the slot acts

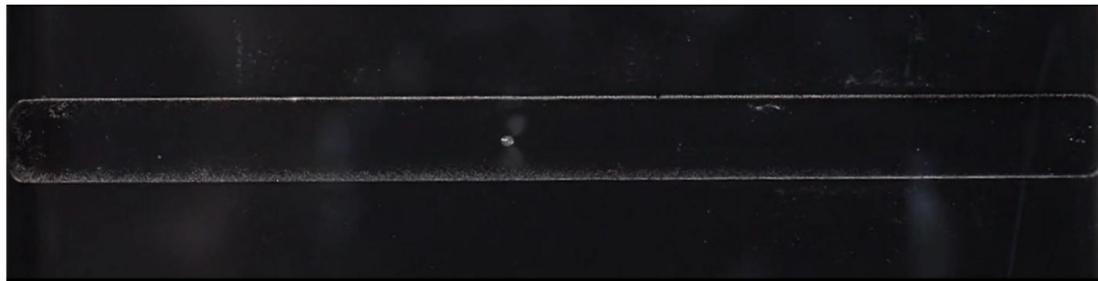


FIG. 1. Top view of a superwalker moving in a submerged channel.

as a damper for Faraday waves. Typically, as the fluid depth increases, the Faraday threshold decreases due to reduced viscous dissipation. In this setup, the fluid depth is 4 mm within the slot and 1 mm outside, creating a significant disparity in Faraday threshold values between these regions. Consequently, the standing waves generated by droplet impacts are rapidly damped outside the slot, preventing the droplet from moving beyond it. Therefore, for the droplet to exhibit walking behavior, it must remain confined within the channel.

In experiments utilizing silicone oil with a kinematic viscosity of 3cSt, the onset of Faraday instability occurred at remarkably low acceleration thresholds, restricting the walking droplet behaviors. In contrast, for the experiment conducted using silicone oil of very high viscosity, the mechanical shaker failed to generate accelerations high enough to trigger the Faraday instability. The optimal viscosity range for our experimental objectives was found to be 20cSt. The experiments conducted in this study, as well as the validation study and the previous work by Valani *et al.*^{17,19} used 20 cSt silicone oil.

The real-time visual data acquisition is realized through a SONY DSLR camera at 50fps. Video analysis is performed using the open-source software TRACKER, which utilizes its particle-tracking algorithm to accurately compute the droplet's velocity and position. Droplets are generated by a rapid upward motion of a toothpick beyond the threshold acceleration for droplet bouncing. The droplet diameter is also computed using image analysis. A typical image of the droplet dynamic captured during our experiments using a high-speed camera is shown in Fig. 2. The droplet is almost spherical during the

flight time which is shown in Fig. 2(a) and the droplet flattens as it interacts with the bath as shown in Fig. 2(b).

For the current study, experiments are conducted for three different harmonic frequency pairs (40, 80), (50, 100), and (70, 140). At lower harmonic frequencies the instability was getting triggered at lower values of acceleration, and studying multiple amplitude ratios was not possible for smaller harmonic frequencies. The harmonic frequency pair of (30, 60) Hz is not suitable for study because of the above reason. At higher harmonic frequencies the bigger droplets were not able to show walking behavior. Also, the Faraday threshold acceleration was very high, and working at higher harmonic frequencies was not feasible due to the inefficiency of the shaker to vibrate at high accelerations. Experiments are conducted for phase angle differences 120°, 130°, 140°, and 150° for all harmonic frequency pairs. Experiments conducted by Valani *et al.*¹⁹ at different phase angle differences concluded that the superwalking behavior was observed for a phase angle difference of 90° to 180° with peak velocity achieved at a phase angle difference close to 140°. This has been observed in our experiments too, which back our results.

The motion of the shaker is monitored using a laser displacement sensor optoNCDT 1420, which can track the movement of the liquid bath over time. The sensor has a precision of 0.001 mm with a measuring rate of 1000 Hz. This enables precise capturing of the movement of the oil bath over time and calculating its acceleration.

The two-channel output function generator as shown in Fig. 3 is connected to the amplifier and the signal can be amplified using the

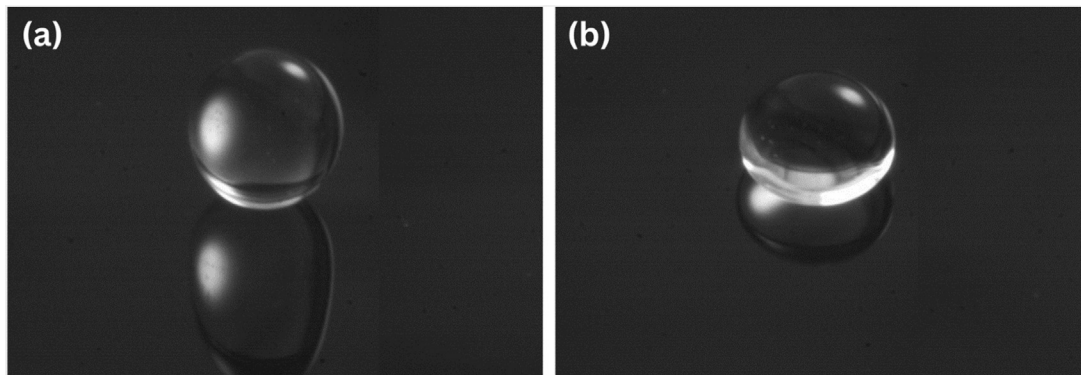


FIG. 2. A superwalker in walking mode: (a) during flight and (b) during contact with the bath.



FIG. 3. Function generator and amplifier.

amplifier gain knob. The amplified signal is connected to the vibration shaker as shown in Fig. 4. The schematic of the experimental facility with all the equipment is shown in Fig. 5.

In all the experiments conducted, the input signal driving the vibrations was a pure sinusoidal waveform represented by the equation $A\sin(2\pi ft + \phi)$. Here, “A” denotes the amplitude of the signal, “f” represents the frequency in Hertz (Hz), “t” is the time variable, and “ ϕ ” signifies the phase angle difference between the two superimposed waveforms. Superwalkers can show completely different behavior when compared to their single-frequency counterparts. This is because of the disparity between the amplitude peaks, which allows the droplets



FIG. 4. Shaker with container mounted on top.

to show superior walking speeds without transitioning into chaotic vertical bouncing. This aspect is shown in Fig. 6 where two sine waves of frequency f and 2f are superimposed.

To ensure the accuracy of the generated waveforms, the quality of the output signal was verified using an oscilloscope. Furthermore, the mechanical vibrations of the liquid bath, induced by the input signal, were monitored and compared with the laser displacement sensor output. This cross-validation approach ensured better control and analysis of the experimental conditions. By employing pure sinusoidal waveforms and verifying the signal quality and mechanical response, the

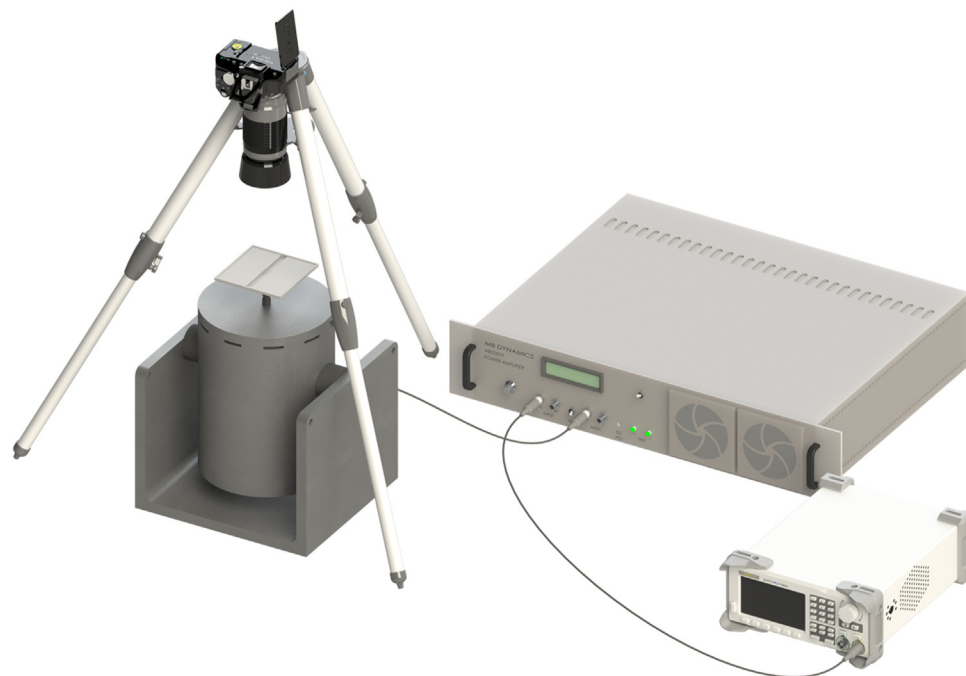


FIG. 5. Schematic diagram of the experimental setup.

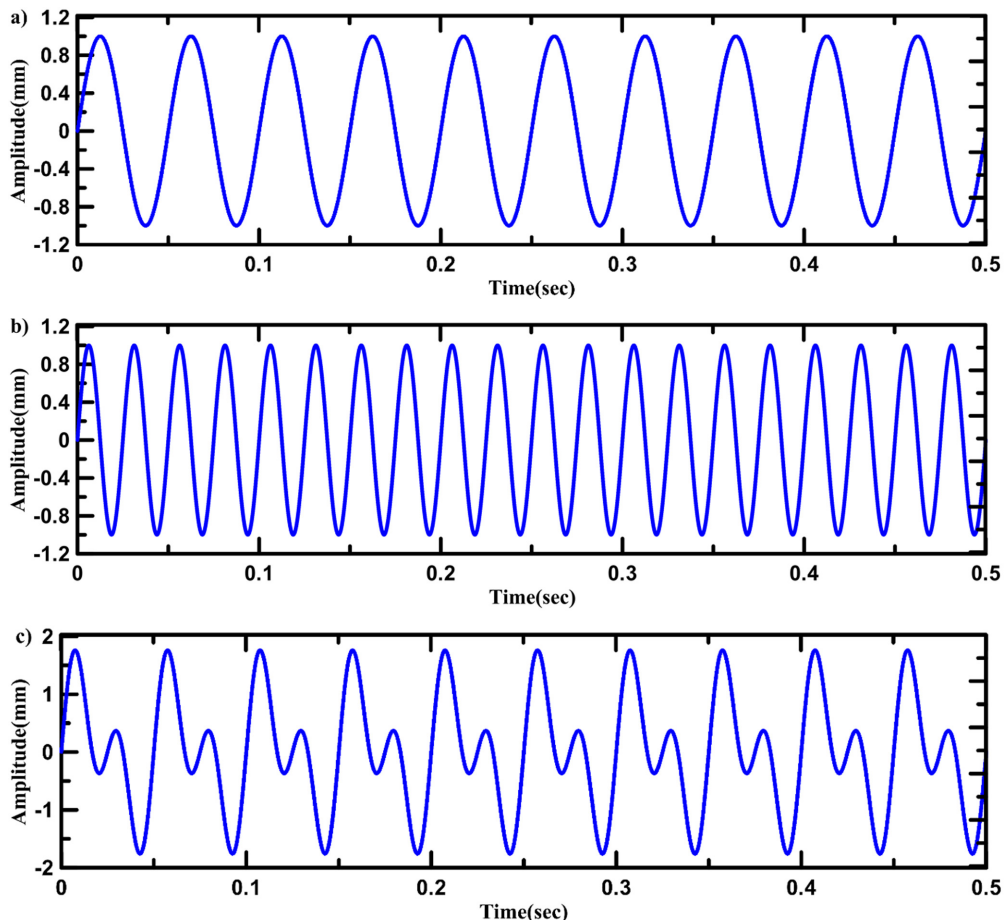


FIG. 6. Representation of (a) sine wave of amplitude 1 and frequency 20 Hz (b) sine wave of amplitude 1 and frequency 40 Hz (c) Superposition of sine waves (a) and (b).

experimental setup maintained a high degree of precision and reliability, thereby facilitating the accurate observation and quantification of the phenomenon associated with the walking droplets and their dynamic behavior.

III. RESULTS AND DISCUSSION

This section discusses the qualitative and quantitative aspects of experimental results. The experiments were conducted for a droplet diameter range of 0.7–2 mm. The harmonic frequency pairs considered are (40, 80), (50, 100), and (70, 140). For each harmonic frequency, the amplitude ratio was varied from 1.0 to 4.5 and the phase angle differences considered are 120°, 130°, 140°, and 150°.

A. Validation results

The experimental setup is validated with the experimental results of Filoux *et al.*¹⁶ The experiments were performed in narrow channels with widths of 1.5λ , 2λ , 4λ , and 5.5λ , where λ represents the wavelength of the Faraday standing waves generated at a frequency of 70 Hz. Both the current study and the work reported by Filoux *et al.*¹⁶ conclude that for channel widths of 1.5λ and 2λ , the trajectories of the

droplets closely approximate a straight line. The droplet moves to and from inside the channel at a constant velocity of 12 mm/s. For containers with comparatively narrower pathways, the droplet motion was observed to follow a straight line trajectory, as illustrated in Fig. 7. However, when the container width exceeded 2λ , the droplet trajectory deviated from a straight line, as depicted in Figs. 7(d) and 7(e). The trajectory paths obtained from Filoux *et al.*¹⁶ corroborate the findings of the current study, wherein it is observed that for channel widths of 4λ and 5.5λ , the droplet trajectory deviates from a straight line.

The to and fro motion of the droplet in the container with near-constant velocity is depicted in Figs. 8(a) and 8(b) along with the results of Filoux *et al.*¹⁶ The X velocity plots of the droplet with a diameter of 0.8 mm in the narrow channel of width 2λ match with the findings reported in the study as shown in Fig. 8(a) validates the current experimental setup.¹⁵ Furthermore, the Y velocity plots, as depicted in Fig. 8(b), reveal that the velocity of the droplets is very close to 0 mm/s, indicating that the droplets are propagating along nearly straight trajectories, which is evident from Fig. 8b. The results obtained in the current study exhibit excellent qualitative and quantitative agreement with those reported by Filoux *et al.*¹⁶

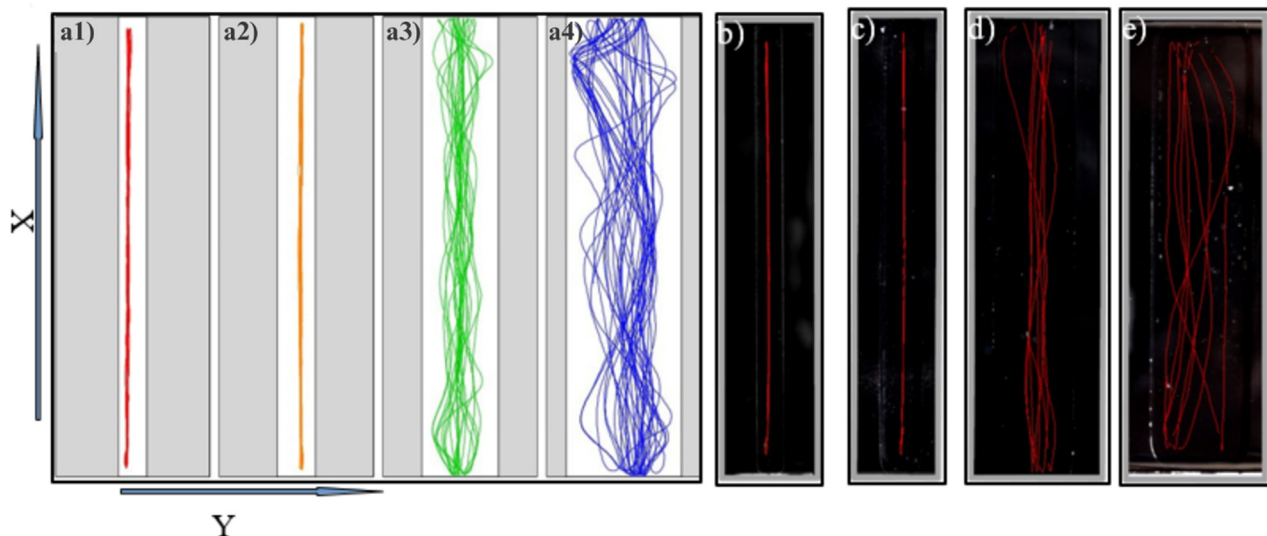


FIG. 7. Trajectory paths of droplet a1) width 1.5λ , a2) width 2λ , a3) width 4λ , and a4) width 5.5λ taken from Filoux et al.¹⁶ (b) Width 1.5λ , (c) width 2λ , (d) width 4λ , and (e) width 5.5λ trajectory paths from the current study (x is the axis along the length of the narrow channel and y is the axis along the width of the narrow channel) (λ is the Faraday wavelength at 70 Hz, which is 5.6 mm) “Reprinted Fig. 7 with permission from Boris Filoux et al., Phys. Rev. Fluids 2, 013601, Volume 2, Issue 1, 2017, Copyright (2017) by the American Physical Society.”

B. Influence of amplitude ratio

In this study, we investigated the behavior of superwalking droplets of diameter range 0.8–2 mm under three distinct harmonic frequency pairs: (40, 80) Hz, (50, 100) Hz, and (70, 140) Hz. We systematically varied the amplitude ratios by incrementally increasing the amplitude of the higher frequency signal by 0.25 units. For each frequency pair and amplitude ratio, we have conducted experiments for phase differences of 120° , 130° , 140° , and 150° .

The amplitude ratio effectively raised the Faraday threshold value, allowing the oil bath to vibrate at greater accelerations without inducing Faraday instability as shown in Fig. 9. For lower frequency

harmonic pairs, although the amplitude ratio is at its maximum, the acceleration is not sufficient to induce walking behavior because Faraday instability is triggered more easily. However, for higher frequency pairs, even with smaller amplitude ratios, the acceleration is adequate to produce walking behavior. As the frequency increases, we observe a broader range of accelerations that can support walking behavior. In all the experiments, the walking acceleration values are above 0.9 times the Faraday threshold values as shown in Fig. 9. The increase in Faraday threshold acceleration for different harmonic frequencies is shown in Figs. 9(a)–9(c). The vertical axis (g^*) represents external acceleration divided by gravitational acceleration.

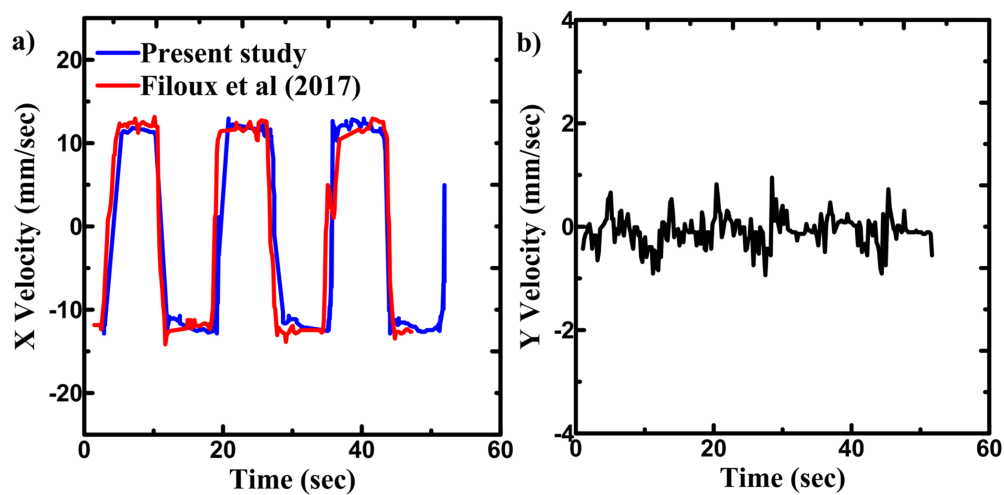


FIG. 8. (a) X velocity of the droplet over time and (b) Y velocity of the droplet over time (present study).

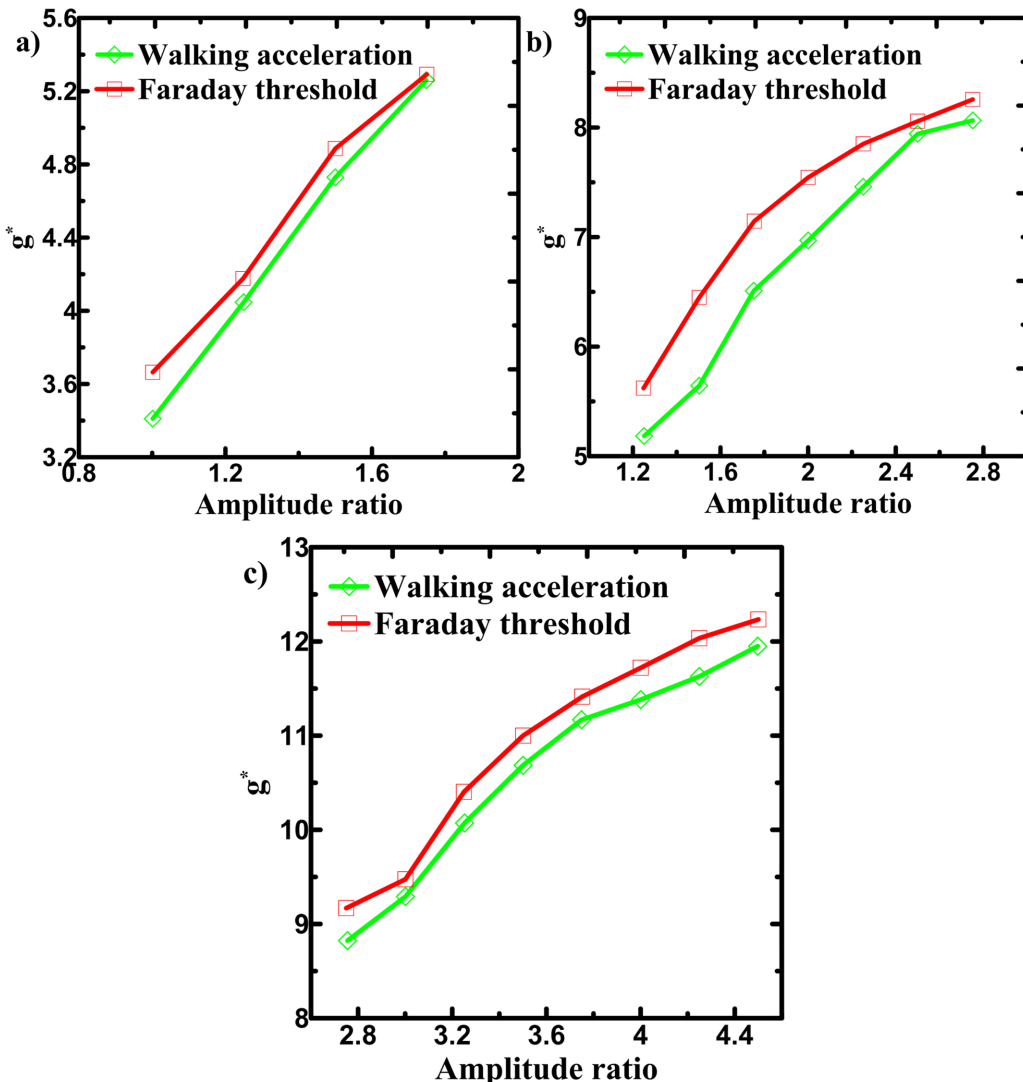


FIG. 9. g^* as a function of amplitude ratio of the input signals comparing walking accelerations of droplets and Faraday threshold acceleration values of the current study: (a) (40, 80) Hz, (b) (50, 100) Hz, and (c) (70, 140) Hz (g^* is a/g where a is the amplitude of external acceleration and g is the acceleration due to gravity).

Our results demonstrate a direct proportional relationship between amplitude ratios and droplet velocity across all harmonic frequencies studied. Higher amplitude ratios led to higher droplet velocities, as evident from Figs. 10(a)–10(c). Notably, we achieved velocities exceeding 60 mm/s for droplets ranging from 1.9 to 2 mm in diameter, surpassing the previously reported maximum velocity of 50 mm/s for a 2 mm droplet for 40–80 Hz. Interestingly, the maximum droplet size exhibiting mobility varied with the harmonic frequency. At (40, 80) Hz, the largest droplet size was 2 mm in diameter, while at 70–140 Hz, the maximum size was reduced to 1.6 mm. Conversely, the smallest droplet sizes capable of walking were 1 mm and 0.7 mm for the (40, 80) Hz and (70, 140) Hz ranges, respectively. At higher harmonic frequencies, the consecutive peaks occurred at smaller time intervals, which affected the (2, 1) bouncing mode of the superwalkers. This shift in the range of effective droplet diameters will be further discussed in Sec. III C.

The range of the acceleration at which superwalking behavior was seen was considerably different at different harmonic frequencies. For the (40, 80) Hz, the amplitude ratio varied from 1 to 1.75 [Fig. 9(a)], corresponding to an acceleration range of 35 m/s^2 to 43 m/s^2 . In the case of 50–100 Hz, the amplitude ratio spanned 1.25 to 2.75 [Fig. 9(b)], resulting in accelerations from 43 m/s^2 to 65 m/s^2 . Furthermore, for the 70–140 Hz ratio, the amplitude varied from 2.75 to 4.5 [Fig. 9(c)], corresponding to accelerations between 80 m/s^2 and 111 m/s^2 . Higher amplitude ratios led to higher accelerations, directly increasing the droplet velocities for all the droplet diameters. When the amplitude ratio is increased from 1.25 to 2.75 for the 50–100 Hz harmonic frequency, a 1.75 mm droplet exhibited an 80% surge in velocity, from 30 mm/s to 54 mm/s [Fig. 10(d)]. Similarly, a 1.55 mm droplet experienced an 82% increase, from 23 mm/s to 42 mm/s [Fig. 10(d)].

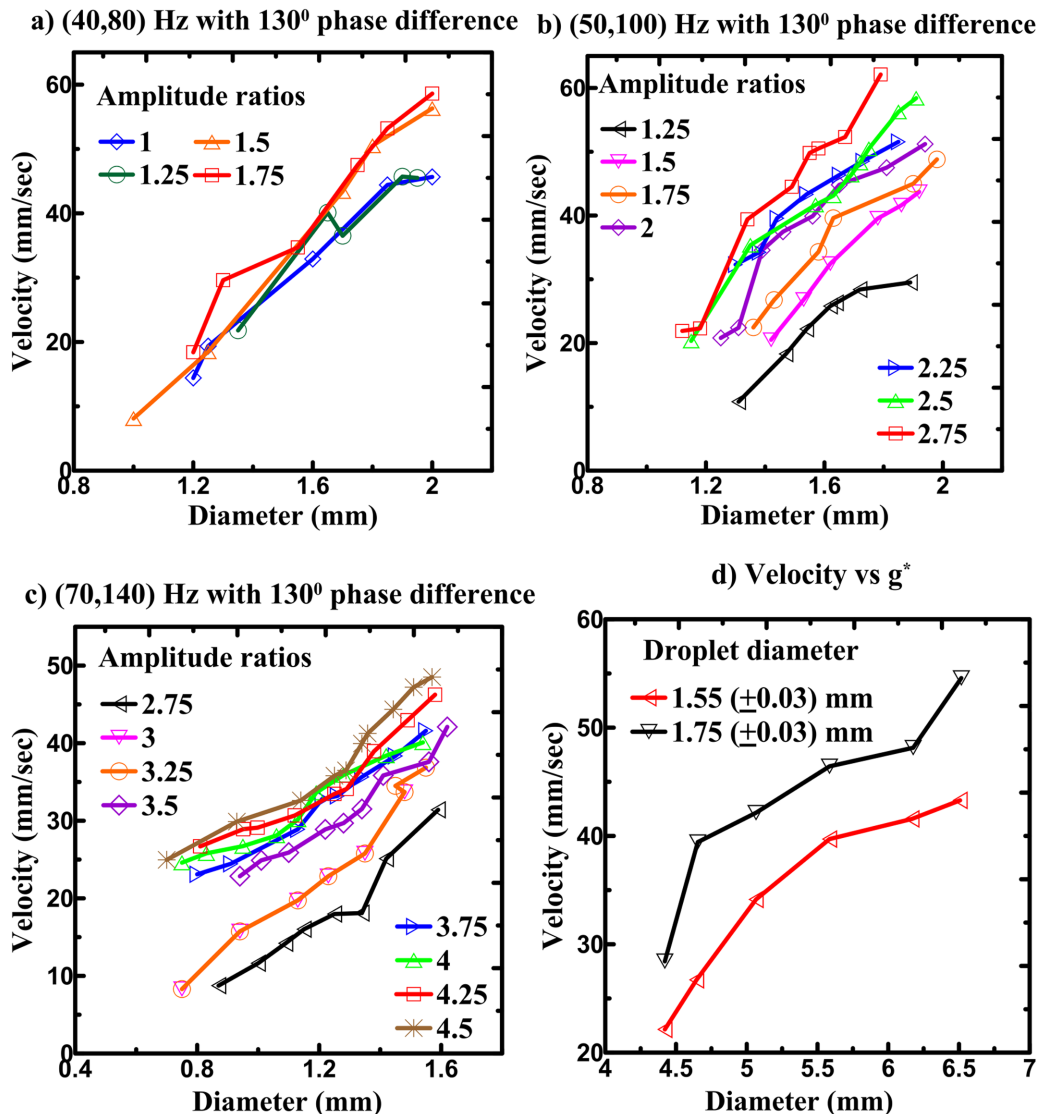


FIG. 10. Droplet velocity as a function of diameter at different amplitude ratios: (a) (40, 80) Hz harmonic frequency, (b) (50, 100) Hz harmonic frequency, (c) (70, 140) Hz harmonic frequency, and (d) droplet velocity as a function of non-dimensional acceleration for droplets of diameters 1.75 and 1.55 mm at (50, 100) Hz harmonic frequency.

All the experiments are repeated for 120° , 130° , 140° , and 150° phase angle differences. At all harmonic frequencies, the droplet has achieved maximum velocities at 130° – 140° and the physics of droplet motion at different phase angle differences are observed to be similar to the results reported by Valani *et al.*¹⁷ Changing phase angle difference changes the adjacent peak-to-peak height of the input signal. For single-frequency forcing, the peaks were of the same height and Valani *et al.*¹⁹ concluded that two-frequency forcing created smaller second peaks for a phase angle difference of 90° to 180° . This enabled bigger droplets to skip the second peak and continue (2, 1) bouncing mode. Since the peak-to-peak height difference is maximum for a phase angle difference of 140° , the droplet achieves maximum velocity for a given frequency and amplitude ratio.

At a particular frequency and droplet size, amplitude ratio helps in achieving a wide range of velocities with good sensitivity. Also, changing the phase difference changes the adjacent peak heights, thereby helping in fine-tuning the velocity further.

To explain the physics of increasing amplitude ratios qualitatively, the displacement sensor images are plotted with possible droplet bouncing motion in Fig. 11. The precise movement of the oil bath, captured using a laser displacement sensor is depicted in Fig. 11(a), (c), and (e), respectively. It focuses on the (50, 100) Hz harmonic frequency pair at a 130° phase angle difference for amplitude ratios of 3.5, 4, and 4.5, with corresponding accelerations plotted in Fig. 11(b), (d), and (f), respectively. On the displacement curves of the vibrating bath, we tried to represent the (2, 1) bouncing mode of the same-sized

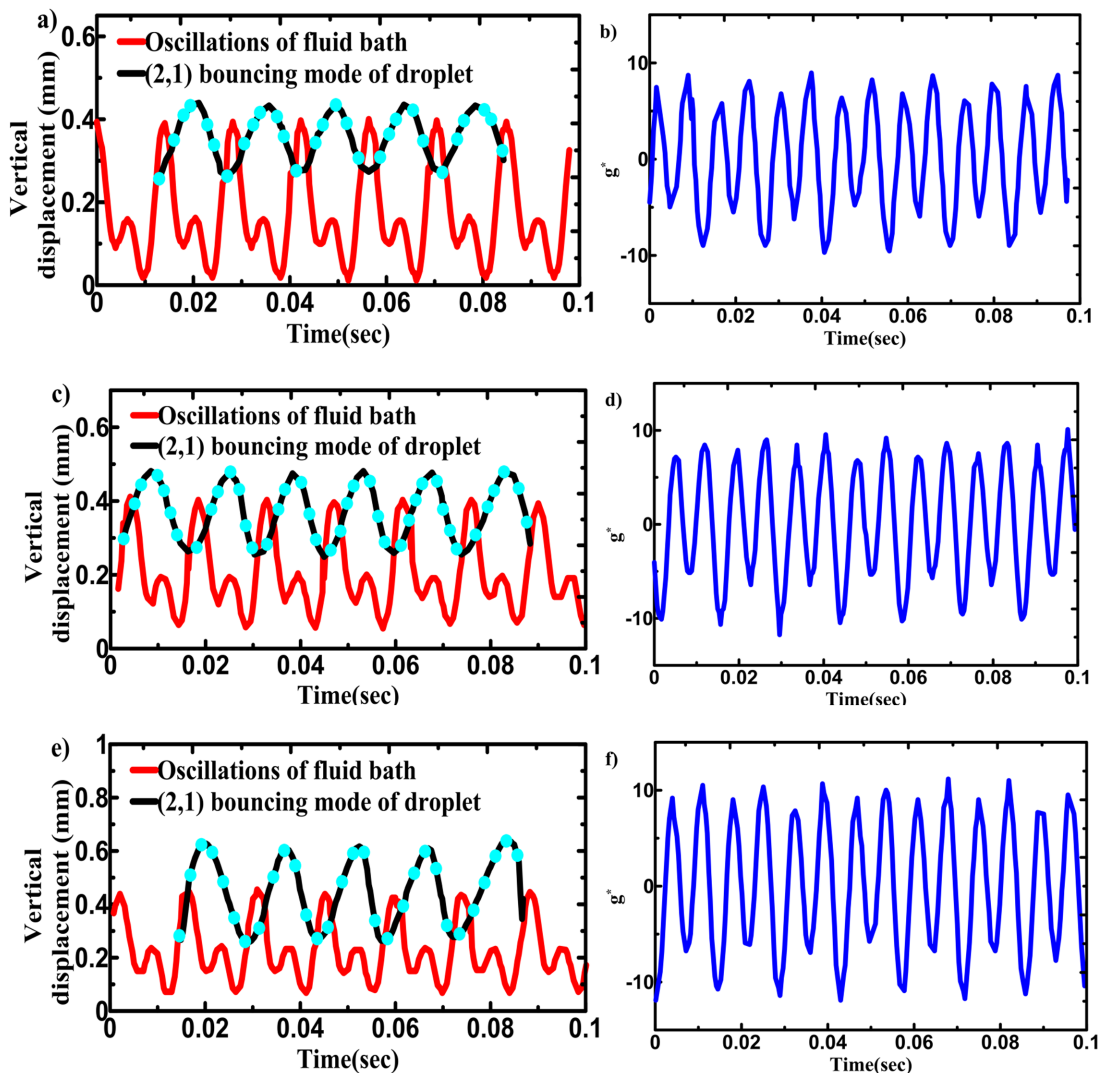


FIG. 11. Representation of the vertical dynamics of liquid droplet of same diameter at (50, 100) Hz and non-dimensional acceleration vs time, (a, b) amplitude ratio 3.5, (c, d) amplitude ratio 4, and (e, f) harmonic frequency 4.5.

droplet to explain the physics with reference to the work reported by Valani *et al.*¹⁷ As the amplitude ratios increased, we observed a consistent maintenance of the peak-to-peak displacement value, with both peaks proportionally increasing while retaining the same overall displacement difference. The droplet's movement, as illustrated in Fig. 11, highlights the importance of maintaining the (2, 1) bouncing mode, where the droplet contacts the oil bath once for every two upward motions of the bath.

Additionally, the utilization of two-frequency forcing with a specific phase angle difference facilitates the droplet's ability to skip the second smaller peak, particularly benefiting larger diameter droplets in achieving a walking behavior. Increasing the amplitude ratio exposes droplets of the same diameter to higher accelerations, possibly making the droplet bounce higher as shown in Figs. 11(a), 11(c), and 11(e).

C. Influence of harmonic frequency

The harmonic frequency had an impact on the range of droplet diameters exhibiting superwalking behavior. At the lower harmonic frequency (40, 80) Hz, the walking droplets had diameters varying from 1 to 2 mm. However, a notable shift occurred when the harmonic frequency was increased to (70, 140) Hz, where the range of walking droplet diameters narrowed significantly to 0.7–1.6 mm. Larger droplets that exhibited walking motion at lower frequencies were unable to maintain their walking behavior when subjected to higher frequencies, despite experiencing a substantial increase in acceleration values as shown in Figs. 12 and 13. Interestingly, this phenomenon was accompanied by an opposing trend observed among smaller droplets. The droplets that initially remained stationary or exhibited chaotic bouncing modes (bouncing without periodicity) at lower harmonic

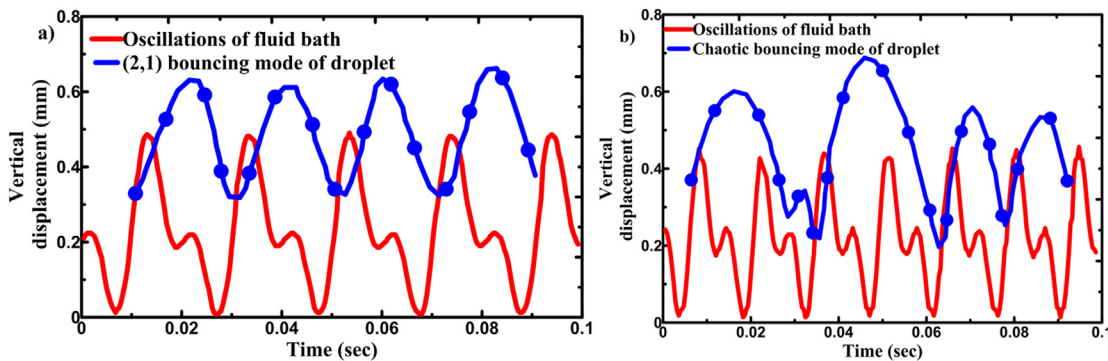


FIG. 12. Representation of vertical dynamics of the droplet motion for larger diameter droplets: (a) 50–100 harmonic frequency and (b) 70–140 harmonic frequency.

frequencies began to exhibit walking behavior when the frequency was increased. Furthermore, these smaller droplets achieved significantly higher velocities compared to their performance at lower frequencies, a direct consequence of the higher accelerations attained due to high-frequency excitations. The size of the droplets that show superwalking characteristics at (40, 80) Hz is 1–2 mm, which shifted to, 0.7–1.7 for (70, 140) Hz. The lower bound on the harmonic frequency at which droplet bouncing is observed depends on the time taken by the air layer trapped between the droplet and liquid bath to escape, which ensures that the droplet never comes in contact with the liquid bath. The upper bound on the frequency range for walking is limited by the time interval between two consecutive peaks and the droplet's ability to sustain the (2, 1) bouncing mode required for walking.

The acceleration of the vibrating bath and the time interval between consecutive higher peaks for the larger diameter droplets at two distinct harmonic frequency pairs: (50, 100) Hz and (70, 140) Hz are shown in Figs. 12(a) and 12(b). Our experimental findings revealed that droplets with a radius of around 1.9 mm exhibited walking behavior at both the (40, 80) Hz and (50, 100) Hz harmonic frequencies. However, droplets of this size range were unable to move at higher frequencies. The time interval between two consecutive higher peaks for (50, 100) Hz harmonic frequency is 0.02 seconds, whereas for (70, 140) Hz harmonic frequency, it is 0.0143 seconds. Because of higher acceleration, the higher frequency, and the peaks occurring at smaller time intervals, the droplet of higher diameter may skip the second consecutive higher peak and is hence unable to maintain the (2, 1) bouncing

mode, which is inevitable for the walking of the droplets as shown in Fig. 12(b).

A similar trend was observed among smaller droplets, which initially did not exhibit walking behavior at lower harmonic frequencies, but demonstrated walking at higher harmonic frequencies. These smaller droplets were bouncing with a chaotic bouncing mode at (50, 100) Hz harmonic frequency as shown in Fig. 13(a). However, when subjected to higher frequencies, the closer consecutive peaks allowed these same-sized droplets to skip the second peak this is evident from Fig. 13(b). The smaller droplets could bounce at (2, 1) mode for lower frequencies. Concluding that if a droplet of diameter of 1 mm is to be moved with higher velocities, parameters should be set at a higher harmonic frequency and amplitude ratio.

Also, increasing frequency did not show any promising increase in the droplet velocities irrespective of the increase in the acceleration of the vibrating bath. However, harmonic frequencies had an important role in deciding the range of droplet diameter it can walk. Higher harmonic frequencies provide more range of acceleration for which the droplet shows superwalking characteristics, which implies better control on the droplet velocities at higher harmonic frequencies, if precise control of the vertical acceleration of the bath is possible. The harmonic frequency gives control over the droplet diameter that can be walked and the amplitude ratio gives control over the droplet velocities. We suggest if a droplet walks at a higher harmonic frequency and a lower harmonic frequency, the higher harmonic frequency is preferred for better control on the velocity. However, if a higher diameter

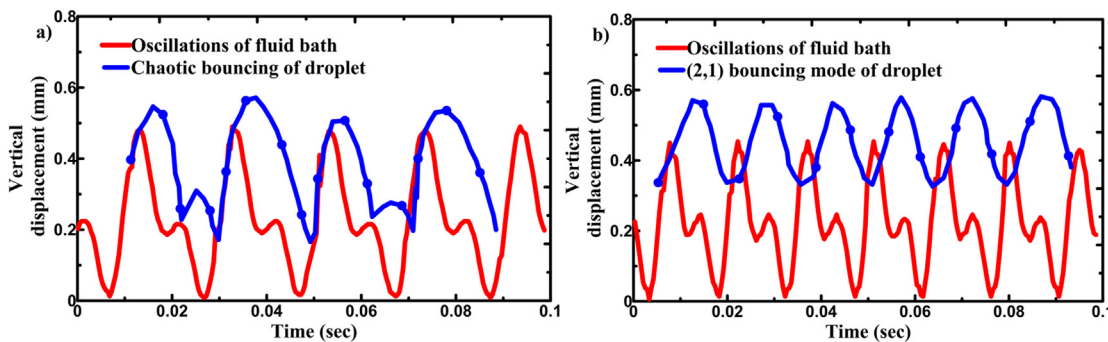


FIG. 13. Representation of vertical dynamics of the droplet motion for smaller diameter droplets. (a) 50–100 Hz harmonic frequency and (b) 70–140 Hz harmonic frequency.

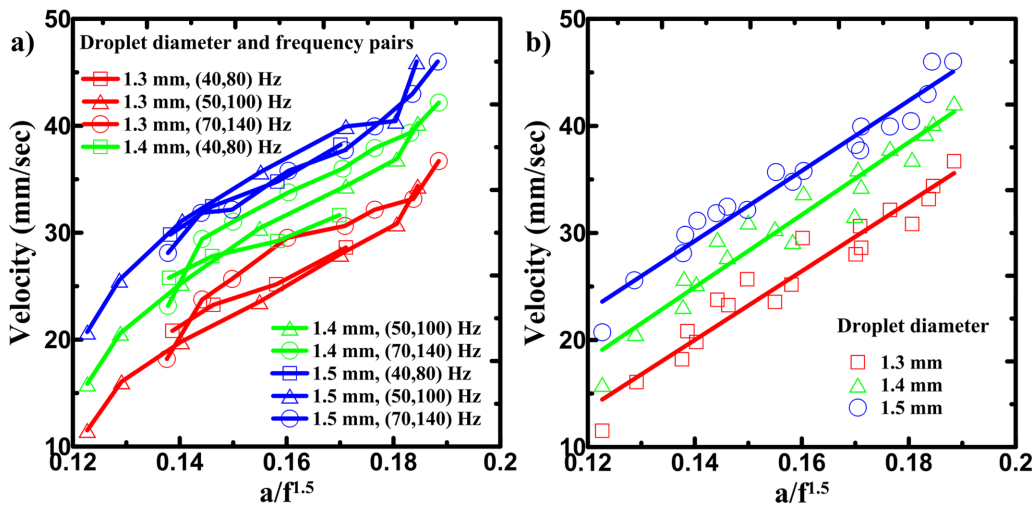


FIG. 14. Droplet velocities as a function of $a/f^{1.5}$. (a is the acceleration and f is the frequency at which droplet is bouncing): (a) diameter of 1.3, 1.4 and 1.5 mm of harmonic frequency (40, 80), (50, 100), and (70, 140) and (b) velocity of droplets of sizes 1.3, 1.4, and 1.5 mm linearly fitted.

droplet is to be walked, comparatively lower harmonic frequencies are preferred.

D. Combined effect of amplitude ratio and harmonic frequency

The combined effect of amplitude ratio and harmonic frequency on the droplet velocity can be explained with a scaling parameter. The experimental data showed promising agreements for different harmonic frequencies when velocities were plotted as a function of $(a/f^{1.5})$. To conclude the combined effect of the harmonic frequency and acceleration on the velocity of the liquid droplet, droplet velocities are plotted as a function of $a/f^{1.5}$ in Fig. 14(a) for droplet diameters 1.3, 1.4, and 1.5 mm and are line fitted as shown in Fig. 14(b). The droplet velocity in Fig. 14(b) shows a good fit with R^2 (coefficient of determinant value) higher than 0.93 in all cases and the maximum percentage error in all three-line fittings was below 10%. The experimental

findings of the current study show that the droplet velocity exhibits a dependency on both the acceleration and the frequency, which can be approximated linearly as a function of the parameter $a/f^{1.5}$. The velocity increases with an increase in diameter as well as $a/f^{1.5}$ ratio. Also, with an increase in 0.1 mm diameter the droplet velocity showed a consistent increment of 5 mm/s, which can be concluded from Fig. 14(b).

E. Influence of radius, frequency, and amplitude ratio on droplet dynamics through the forces acting on the droplet

The effect of various parameters like radius, frequency, driving acceleration, and amplitude ratio on the walking behavior can be understood with the help of forces as shown in Fig. 15 acting on the droplet and their variation w.r.t these parameters.¹¹ A non-dimensional version of the magnitude of these forces is discussed to

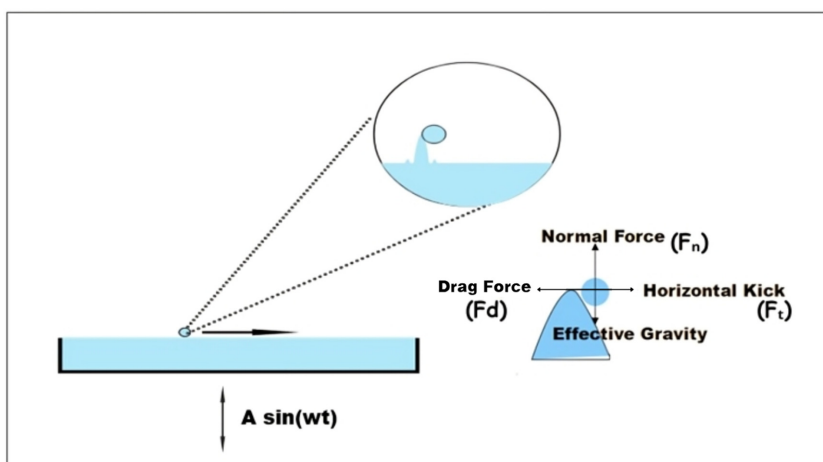


FIG. 15. Schematic of a droplet bouncing on a vertically vibrating liquid bath above walking threshold acceleration (droplet size is exaggerated for better visibility).

understand the true effect of these parameters.¹¹ The various forces acting on the droplet at the time of contact while walking are:

- (1) **Horizontal drag due to pressure gradient:** When the drop makes an oblique impact on the bath, it leads to non-axisymmetric deformation of the droplet. Experimentally, it is observed that because of the horizontal momentum imparted to the air, a horizontal pressure gradient appears in the air film due to the inertia of the air. This is the major opposing force for walking. Experimentally, it is hypothesized that this force scales as $(F_d \sim C \cdot F_n \cdot X_t)$, where C is some constant whose value is typically 0.3, F_n is the vertical reaction force applied by the bath (mediated by air), and X_t is the non-dimensional horizontal velocity.
- (2) **Shear drag in the intervening layer and Stokes drag:** Because of the variation in the horizontal velocity of air in the contact region, there will be a shear force on the drop. But its magnitude is very low compared to horizontal drag due to the pressure gradient. During the flight, since horizontal velocity is not high, drag force can be approximated with the help of creeping flow approximation. So, it scales as $(F_d \sim Oh_a \cdot X_t)$, where Oh_a (Ohnesorge number) = $\mu_a / \sqrt{\rho \sigma R_0}$. (μ_a being the dynamic viscosity of air, R_0 is the droplet radius)
- (3) **Horizontal kick by the bath:** This is the driving force that propels the droplet forward. When the drop lands on the crest of the slowly decaying standing waves of the bath, a horizontal force acts on the drop, which is mediated by the pressure of air. If the total net force acting on the drop is in the normal direction of the bath, then the horizontal kick force scales as $F_t \sim h_x \cdot F_n$ where h_x is the x-derivative of the bath surface height.

The walking motion results from a competition between these forces. Initially, any horizontal perturbations are suppressed by these two forces. However, once the walking threshold is reached, the slowly decaying standing waves generated during impact begin to destabilize the purely vertical bouncing motion, allowing the droplet to exhibit walking behavior.

Walking behavior cannot be seen in droplets that are either small or too large for a certain frequency. There exists an optimum radius at which a minimum walking threshold is achieved. If the radius is small, mostly it will end up in a chaotic vertical motion because of the larger vertical reaction force. Since Stokes drag will be larger for smaller droplets and drag due to pressure gradient will also be high due to large reaction force, smaller droplets do not show walking behavior. Larger droplets tend to switch to lower energy modes because of their relatively higher contact time due to larger deformation, hence the driving reaction force is too small to show walking behavior. Typically, the walking regime is bordered between chaotic bouncing states. That is why too small and too large droplets do not show walking behavior.

Smaller droplets begin to walk as the frequency rises because the bath's horizontal kick increases as the standing wave decay rate ($a/a_f - 1$) drops and the vertical reaction force rises as a result of reduction in contact time (where "a" is the driving acceleration and " a_f " is the Faraday threshold)¹¹ Because of the internal dissipation effects caused by increased horizontal forces, the larger droplets are unable to survive in the (2, 1) mode and instead transition to lower energy modes, which lowers the upper constraint on the radius at which the walking behavior is observed. This effect is predominant in superwalkers.

With the increase in frequency, the strength of the wave-field (due to the decrease in decay rate because both walking acceleration and Faraday threshold increase) and the normal reaction force increase, which enhances the velocity of the droplet significantly even though drag increases. A similar effect is observed when the amplitude ratio is raised because its net effect will raise the driving acceleration. Velocity initially increases with an increase in radius due to an increase in reaction force applied by the bath, then shows an abrupt trend due to a change in bouncing mode, finally leading to coalescence.

IV. CONCLUSION

The velocity of walking droplets on a vibrating liquid bath exhibits a dependency on the harmonic frequency and amplitude ratio of the vibrating bath. It has been observed that an increase in the amplitude ratio leads to a corresponding increase in the droplet velocity. The amplitude ratio helps in adjusting the velocity as per the requirement and phase angle can be used for fine-tuning.

Through precise control of the amplitude ratio, it has been possible to achieve droplet velocities as high as 60–65 mm/s, surpassing the previously reported maximum velocity of 50 mm/s in earlier studies. Furthermore, the harmonic frequency has been found to influence the range of droplet diameters that exhibit walking behavior. For higher harmonic frequencies in the range of (70, 140) Hz, the maximum droplet size that can sustain walking motion is reduced to a diameter of 1.6 mm and it has been concluded that smaller droplets in the range of 0.7 mm diameter can show superwalking behavior at higher harmonic frequencies. So, the droplet size dictates the optimum frequency based on the ability to sustain (2, 1) bouncing mode and available acceleration range.

When plotted for a single-diameter droplet, experimental data show good linear agreements between velocity with $a/f^{1.5}$ ratio. This functional relationship explains the combined influence of acceleration and harmonic frequency on droplet velocity dynamics giving more control of superwalker velocities.

ACKNOWLEDGMENTS

The authors acknowledge Science & Research Board (SERB) for the financial support (order no CRG/2022/003494) and Department of Science and Technology India, FIST project No (SR/FST-II/2017/100).

AUTHOR DECLARATIONS

Conflict of Interest

The authors have no conflicts to disclose.

Author Contributions

P. P. Pranav: Conceptualization (equal); Data curation (equal); Formal analysis (equal); Investigation (equal); Methodology (equal); Software (equal); Validation (equal); Visualization (equal); Writing – original draft (equal). **Pranay Prabha Badvelu:** Data curation (equal); Formal analysis (equal); Investigation (equal); Writing – review & editing (equal). **Venugopal Arumuru:** Conceptualization (equal); Formal analysis (equal); Funding acquisition (equal); Investigation (equal); Methodology (equal); Project administration (equal); Resources (equal); Supervision (equal); Validation (equal); Visualization (equal); Writing – original draft (equal).

DATA AVAILABILITY

The data that support the findings of this study are available from the corresponding author upon reasonable request.

REFERENCES

- ¹M. Faraday, "On a peculiar class of acoustical figures; and on certain forms assumed by groups of particles upon vibrating elastic surfaces," *Philos. Trans. R. Soc. London* **121**, 1 (1831).
- ²S. Douady and S. Fauve, "Pattern selection in Faraday instability," *Europhys. Lett.* **6**(3), 221 (1988).
- ³C. S. Tsai, R. W. Mao, S. C. Tsai, K. Shahverdi, Y. Zhu, S. K. Lin *et al.*, "Faraday waves-based integrated ultrasonic micro-droplet generator and applications," *Micromachines* **8**(2), 56 (2017).
- ⁴N. Singh and A. Pal, "Quantifying the turbulent mixing driven by the Faraday instability in rotating miscible fluids," *Phys. Fluids* **36**(2), 024116 (2024).
- ⁵T. B. Benjamin and F. Ursell, "The stability of the plane free surface of a liquid in vertical periodic motion," *Proc. R. Soc. London A* **225**(1163), 505 (1954).
- ⁶K. Kumar and L. S. Tuckerman, "Parametric instability of the interface between two fluids," *J. Fluid Mech.* **279**, 49–68 (1994).
- ⁷K. Kumar, "Linear theory of Faraday instability in viscous liquids," *Proc.: Math., Phys. Eng. Sci.* **452**(1948), 1 (1996).
- ⁸H. Arbell and J. Fineberg, "Pattern formation in two-frequency forced parametric waves," *Phys. Rev. E* **65**(3), 036224 (2002).
- ⁹Y. Couder, S. Protière, E. Fort, and A. Boudaoud, "Walking and orbiting droplets," *Nature* **437**, 208 (2005).
- ¹⁰J. W. Bush, "Pilot-wave hydrodynamics," *Annu. Rev. Fluid Mech.* **47**, 269–292 (2015).
- ¹¹J. Molacek and J. W. M. Bush, "Drops walking on a vibrating bath: Towards a hydrodynamic pilot-wave theory," *J. Fluid Mech.* **727**, 612–647 (2013).
- ¹²J. Molacek and J. W. M. Bush, "Drops bouncing on a vibrating bath," *J. Fluid Mech.* **727**, 582–611 (2013).
- ¹³D. M. Harris, J. Moukhtar, E. Fort, Y. Couder, and J. W. M. Bush, "Wavelike statistics from pilot-wave dynamics in a circular corral," *Phys. Rev. E* **88**, 011001 (2013).
- ¹⁴A. Nachbin, P. A. Milewski, and J. W. M. Bush, "Tunneling with a hydrodynamic pilot-wave model," *Phys. Rev. Fluids* **2**, 034801 (2017).
- ¹⁵S. Perrard, M. Labousse, M. Miskin, E. Fort, and Y. Couder, "Self-organization into quantized eigenstates of a classical wave-driven particle," *Nat. Commun.* **5**, 3219 (2014).
- ¹⁶B. Filoux, M. Hubert, P. Schlagheck, and N. Vandewalle, "Waveguides for walking droplets," *Phys. Rev. Fluids* **2**, 013601 (2017).
- ¹⁷R. N. Valani, A. C. Slim, and T. Simula, "Superwalking droplets," *Phys. Rev. Lett.* **123**, 024503 (2019).
- ¹⁸R. N. Valani, A. C. Slim, and T. Simula, "Stop-and-go locomotion of superwalking droplets," *Phys. Rev. E* **103**, 043102 (2021).
- ¹⁹R. N. Valani, J. Dring, T. P. Simula, and A. C. Slim, "Emergence of superwalking droplets," *J. Fluid Mech.* **906**, A3 (2021).